

## **AN INVESTIGATION ON SOME DESIGN PARAMETERS IN FREE SPACE OPTICAL COMMUNICATION BETWEEN ON-SEA TERMINALS**

F. OZEK

*Dept. of Electronics, Faculty of Science, 06100 Tandoğan, Ankara, Turkey.*

(Received June 6, 2000; Accepted Sep 11, 2000 )

### **ABSTRACT**

Maximum free space optical communication distances between mobile on-sea terminals, by night, are numerically evaluated for 2.4 to 57.6 kbps bit rates and clear and hazy weather conditions. Advantages of a medium power laser diode at the transmitter are pointed out. Effects of other design parameters such as the use of an optical filter, the size and position of the laser spot on the receiver four-quadrant detector are analysed.

### **1. INTRODUCTION**

Contrary to the fact that almost all the laser applications take advantage of the narrow beam divergence of the laser, in free space optical communication, FSOC, between mobile terminals, the transmitter laser beam divergence angle has to be widened up to  $35^\circ$ , the line-of-sight requirement still being a must [1]. In this paper, on-sea FSOC applications, i.e. from ship to ship, are numerically analyzed. Justification for using a wide angle laser beam in such applications is the fact that both the transmitter and receiver ships are in three dimensional motion, i.e. vertical and sidewise movements are added to the direction of motion, so that the probability of detection would be almost zero if a narrow beam laser were employed. The wide beam divergence angles of medium power laser diodes, normally a disadvantage, fulfil this requirement.

### **2. MEDIUM POWER LASER DIODES**

An investigation on the commercially available laser sources will indicate that a power output around and above 100 mW can be accepted to typify the medium power laser diodes, MPLD. Moreover, the MPLD emission exhibits an elliptic profile so that  $\theta_{//}$  and  $\theta_{\perp}$  are the parallel and perpendicular divergence angles, corresponding to the minor and major axes of the elliptic beam, respectively. The advantage of using an elliptic beam at the transmitter, therefore, is the fact that the vertical movements of on-sea terminals are much less than the horizontal motion which exactly fits to the elliptic nature of the beam when the major axis of the ellipsis is adjusted horizontally.

On-land applications, however, the vertical deviations between the transmitter and receiver are likely to be considerably high and a circular beam may be more practical. An elliptic beam can be circularized by using an anamorphic prism pair in front of the laser diode, which expand the minor axis of the elliptic output so as to make the circular divergence angle  $\theta = \theta_{\perp}$ .

In this work, the maximum communication distances, the ultimate measure of performance, have been numerically obtained, for different bit rates and weather conditions, assuming a commercially available MPLD of  $P = 150 \text{ mW}$ ,  $\theta_{//} = 7^{\circ}$ ,  $\theta_{\perp} = 17^{\circ}$ ,  $\lambda = 0.830 \mu$ , used at the transmitter.

The laser intensities,  $\phi$ , in terms of Watts per  $\text{m}^2$ , at a distance  $R$  from the source are given by equations (1) and (2) for elliptic and circular beam profiles, respectively.

$$\phi_e = P \exp(-\tau R) / \pi R^2 (\tan \theta_{\perp} : 2) (\tan \theta_{//} : 2) \quad \text{W} / \text{m}^2 \quad (1)$$

$$\phi_c = P \exp(-\tau R) / \pi R^2 \tan^2 \theta / 2 \quad \text{W} / \text{m}^2 \quad (2)$$

where  $P$  : laser power,  $W$

$\tau$  : atmospheric attenuation coefficient,  $\text{m}^{-1}$   
 $= 2 \times 10^{-4} \text{ m}^{-1}$  for clear weather  
 $= 1 \times 10^{-3} \text{ m}^{-1}$  for hazy weather [2]

$R$  : distance from the source,  $m$

Although the Gaussian profile of the laser output flattens out in the far field, 86% of the power is taken in to account [3], not the nominal power rating of  $P = 150 \text{ mW}$ .

### 3. RECEIVER

The basic receiver components are depicted in Figure 1. The signal carrying laser rays from the transmitter pass through a narrow band, laser line optical interference filter  $F$ , and are collected and focused by a thin lens  $L$ , onto the four-quadrant 4Q detector which simultaneously senses (detects) the laser signal and produces the deviation data required for tracking the transmitter by the receiver and pointing its own laser beam towards the transmitter [4].

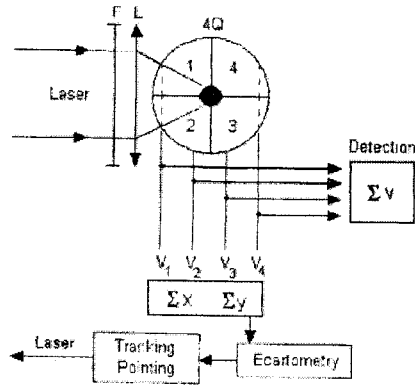


FIGURE 1

The laser signal collected on the 4Q is not a fine point but an intentionally defocused spot so as to make deviation measurements possible. Moreover, there is an insensitive region (gap), width  $d$ , separating the quadrants. If the spot is contained within any of the quadrants then the full laser energy will be sensed. However, especially when the spot is located in the center of the 4Q, i.e. the transmitter is on the receiver axis, the detected laser energy will be less by the "detectable area factor", defined in this work, DAF% as formulated very approximately in equation (3).

$$\text{DAF}\% = (a-d) (a-1.5 d) / a^2 \quad (3)$$

Where  $a$  : laser spot size (diameter)  
 $d$  : insensitive gap width

For  $a = 2.8$  mm, DAF% is obtained from equation (3) as 83%. The receiver parameters, based on the commercially available component data and used in the present evaluations are listed in Table 1.

Table 1. Receiver Components and Parameters

| Component      | Parameter   |
|----------------|---|
| Optical filter | Transmission $F\% = 50\%$ $\Delta\lambda = 10$ nm   |
| Lens           | Dia = 25 mm $S(\text{opt}) = 4.9$ cm <sup>2</sup> $f = 24.7$ mm   |
| 4Q             | Dia $A = 11.3$ mm, $d = 0.2$ mm<br>Responsivity $\sigma = 0.5$ Amp/W (at $\lambda = 0.830\mu$ )<br>Dark current $I(d) = 50$ nA, max |

#### 4. SIGNAL

The relationship which gives the signal current  $i(S)$ , either for elliptic or circular beam, is given in equation (4).

$$i(S) = \phi F\% S(\text{opt}) \text{DAF}\% \sigma \quad \text{Amp} \quad (4)$$

where

- $\phi$  : laser intensity,  $\text{W/m}^2$
- $F\%$  : optical filter transmission, %
- $S(\text{opt})$ : optical (lens) area,  $\text{m}^2$
- $\sigma$  : 4Q responsivity,  $\text{Amp/W}$

#### 5. NOISE

The total noise current  $i(N)$  is the sum of the detector (shot) noise  $i(d)$ , resulting from the dark current  $I(d)$  plus the background, (BG), noise  $I(b)$ , and the detector load resistance noise  $i(R_L)$ , which are given in Equations (5), (6) and (7), respectively.

$$i(N) = [ i^2(d) + i^2(R_L) ]^{1/2} \quad (5)$$

$$i(d) = [ 2e [ I(d) + I(b) ] \Delta f ]^{1/2} \quad (6)$$

$$i(R_L) = (4 k T \Delta f / R_L)^{1/2} \quad (7)$$

where

- $e = 1.6 \times 10^{-19}$  Coulomb
- $I(d)$ : dark current
- $I(b)$ : BG current
- $\Delta f$ : bandwidth, Hz
- $k$ : Boltzmann's constant =  $1.38 \times 10^{-23}$   $\text{J}^\circ\text{K}$
- $T = 293$   $^\circ\text{K}$  ( $20^\circ\text{C}$ )
- $R_L$ : load resistance =  $200 \text{ k}\Omega$

By night, the only source of the ambient BG noise,  $I(b)$ , is the ground self-infrared emission, which can be assessed using the well-known Planck's law given in equation (8), [5].

$$W(\lambda) = 2\pi hc^2 \lambda^{-5} / \exp(hc / \lambda kT) - 1 \quad \text{W cm}^{-2} \mu^{-1} \quad (8)$$

where  $h$ : Planck's constant =  $6.63 \times 10^{-34}$   $\text{J}\cdot\text{sec}$

$$\begin{aligned}
 c &= 3 \times 10^{10} \text{ cm / sec} \\
 \lambda &= 0.830 \mu \\
 T &= 293 \text{ }^\circ\text{K}
 \end{aligned}$$

In this work equation (8) is re-written considering the optical filter bandwidth  $\Delta\lambda$  and the more practical steradian, sr, unit as given in equation (9).

$$dW(\lambda) = \Delta\lambda (1.2 \times 10^4) \lambda^{-5} / \exp(14394 / \lambda T) - 1 \quad \text{W cm}^{-2} \text{ sr}^{-1} \quad (9)$$

where  $\Delta\lambda$  : optical filter bandwidth,  $\mu$

The corresponding BG current is obtained from equation (10) to be  $I(b) = 2 \times 10^{-25}$  Amp which is well below the 4Q dark current ( $I(d) = 50 \text{ nA}$ , therefore negligible.

$$I(b) = dW(\lambda) \Omega(\text{rec}) F(\%) S(\text{opt}) \sigma \quad \text{Amp} \quad (10)$$

where

$$\begin{aligned}
 \Omega(\text{rec}) &: \text{receiver solid angle, } 0.09 \text{ sr} \\
 &= 2\pi(1 - \cos \text{FOV}/2)
 \end{aligned}$$

$$\begin{aligned}
 \text{FOV} &: \text{receiver field-of-view} \\
 &= 2 \arctan((A - a) / 2f)
 \end{aligned}$$

The total noise current, for example at 57.6 kbps ( $\Delta f = 2.88 \times 10^4 \text{ Hz}$ ), i.e. speech communication, and for  $R_L = 200 \text{ k}\Omega$ , is  $i(N) = 5.3 \times 10^{-11} \text{ Amp}$ .

## 6. SIGNAL-TO-NOISE RATIO, SNR

The Infrared Data Association IrDA specification states that the bit error rate BER shall be no greater than  $10^{-8}$ . In this work the BER is set to  $10^{-9}$  which yields a threshold SNR of 72 by equation (11), when the frequency shift keying FSK is assumed to be used in the communication,

$$\text{BER} = Q(\text{SNR} / 2)^{1/2} \quad (11)$$

where  $Q$  is the Gaussian  $Q$  function which is 6 for the BER of  $10^{-9}$ , [6].

## 7. RESULTS AND DISCUSSION

The variation of the maximum communication distance  $R_{\text{max}}$  with the bit rate for clear and hazy weather conditions are presented in figures 2 and 3. Practically useful distances are exhibited especially for closely sailing ships. Although the distances are on the average 100 m longer for the elliptic beam, a circular beam can be advantageous in on-land applications, i.e. between vehicles, where high vertical deviations between the terminals can be encountered.

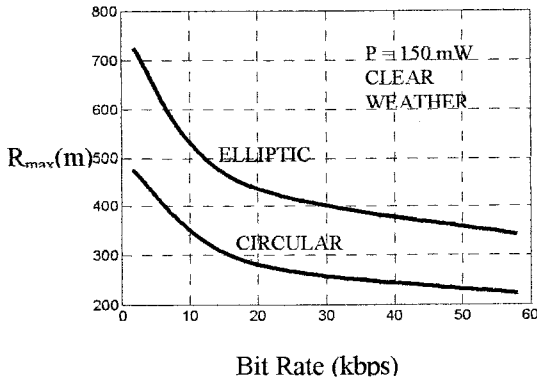


FIGURE 2

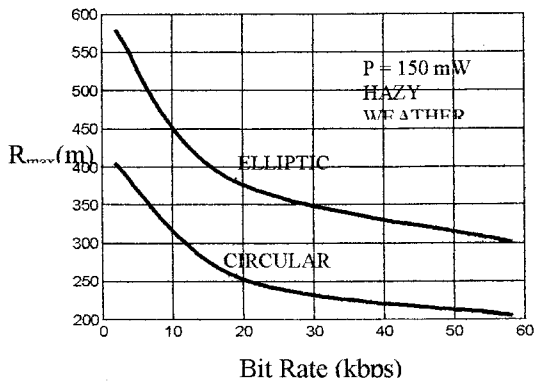
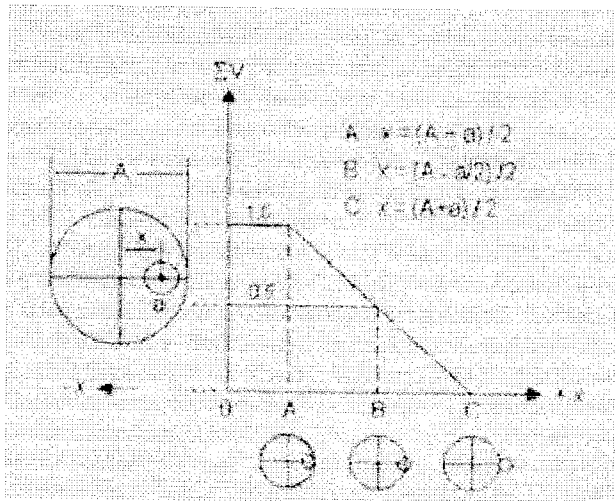


FIGURE 3

By night, the only "impulse" noise may be the strong infrared emission from the lightning strokes [7]. Considering the low probability of occurrence of such an impulse noise, an optical filter may not be used in the receiver. The received signal is therefore increased, which results in longer  $R_{max}$  values, as indicated in Table 2. It can be seen that at 57.6 kbps and for clear weather,  $R_{max}$  is nearly half a kilometer, for the elliptic beam.

Table2.  $R_{\max}$  without optical filter  
(57.6 kbps)

| Atmospheric Condition | $R_{\max}$ (m) |          |
|-----------------------|----------------|----------|
|                       | Circular       | Elliptic |
| Clear                 | 270            | 473      |
| Hazy                  | 245            | 407      |



(FIGURE 4)

Figure 4 illustrates the effect of the laser spot position on the 4Q detector. Up to the position A, the full laser signal, corresponding to  $\Sigma V = V_1 + V_2 + V_3 + V_4$ , is detected. At B, the 4Q output is 50% lower, i.e.  $0.5 \Sigma V$ . Although at this half-power detection position  $R_{\max}$  decreases, the FOV widens, resulting in an increased time for the tracking that is important where the terminals are at relatively high speeds.

Although the tracking aspect of such a system could not be included in the scope of this paper, the detailed information on tracking using a 4Q detector can be found in the literature [4].

## REFERENCES

- [1] Photonics Spectra, July, (1993), p. 16.
- [2] MOLLIE, P. and CHABANNES, F. : NATO-AGARD, Lecture Series on Opto-Electronics, LS-71, (1974), p.8-1.

- [3] SALEH, M.B.A. and TEICH, M.C.: *Fundamentals of Photonics*, (Wiley, New York, 1991), p.85.
- [4] GAGLIARDI, R. and KARP, S.: (*Optical Communications*, Wiley, New York, 1995), p.324.
- [5] WATSON, J.; *Optoelectronics*, (Van Nostrand Reinhold Co. Ltd, Wokingham, UK, 1988), p.143.
- [6] CARLSON, A.B.: *Communication Systems*, (Mc Graw-Hill, London, 1986), p.666.
- [7] ORVILLE, R.E. and HENDERSON, R.W.: *J. Atmospheric Sciences*, 41, (1984), 3180.